PREDICTIVE MODEL FOR TOLUENE DEGRADATION AND MICROBIAL PHENOTYPIC PROFILES IN FLAT PLATE VAPOR PHASE BIOREACTOR

By Raj Mirpuri,[1] Warren Sharp,[2] Santiago Villaverde,[3] Warren Jones,[4] Zbigniew Lewandowski,[5] and Al Cunningham[6]

ABSTRACT: A predictive model has been developed to describe degradation of toluene in a flat-plate vapor phase bioreactor (VPBR). The VPBR model incorporates kinetic, stoichiometric, injury, and irreversible loss coefficients from suspended culture studies for toluene degradation by *P. putida* 54G and measured values of Henry's law constant and boundary layer thickness at the gas-liquid and liquid-biofilm interface. The model is used to estimate the performance of the reactor with respect to toluene degradation and to predict profiles of toluene concentration and bacterial physiological state within the biofilm. These results have been compared with experimentally determined values from a flat plate VPBR under electron acceptor and electron donor limiting conditions. The model accurately predicts toluene concentrations in the vapor phase and toluene degradation rate by adjusting only three parameters: biomass density and rates of death and endogenous decay. Qualitatively, the model also predicts gradients in the physiological state cells in the biofilm. This model provides a rational design for predicting an upper limit of toluene degradation capability in a VPBR and is currently being tested to assess applications for predicting performance of bench and pilot-scale column reactors.

INTRODUCTION

Vapor phase bioreactors, or biofilters as they are commonly known, have been used to treat relatively low concentrations of highly odorous compounds and potential air pollutants such as volatile organic compounds produced by industrial processes, waste treatment and domestic activities (Leson and Winer 1991). Recent amendments to the Clean Air Act have increased the level of interest in treating contaminated air streams using biofilters because they offer a low-cost and low-maintenance alternative to other air pollution control technologies. The traditional approach of treating vapor phase bioreactors (VPBRs) as a black box for remediation of contaminated gases has produced promising results in some cases, but from a process control standpoint, this technology is still in the early phase of development. Design and control strategies in reference to packing characteristics, biofilm processes, loading rates, reactor plugging, medium pH, pressure drop, and oxygen content are necessary. Traditional biofilter design and operation have been carried out without detailed studies on biofilm processes within VPBRs. Biofilm processes leading to substrate degradation and subsequent cell growth are critical to the performance of VPBRs. Processes of reaction and diffusion in VPBRs are complicated because they involve diffusion from the bulk gas layer through a stagnant liquid layer into the biofilm where substrate degradation occurs. As biofilm thickness increases, mass transfer limitations for both electron acceptor and electron donor may occur, leading to the formation of anaerobic zones and/or dead cells within the biofilm. Other processes such as bacterial injury and toxicity due to degradation of volatile organic compounds are not well understood. These processes are extremely important for assessing steady-state performance of VPBRs. Scale up of VPBRs can best be achieved through use of predictive models, the success of which depends on accurate estimates of kinetic, stoichiometric, and mass transfer coefficients.

Most models developed for predicting VPBR performance have used simplifying assumptions regarding degradation kinetics or mass transfer resistance. Diks and Ottengraf (1991) developed a simplified model to describe the removal of dichloromethane from a biological trickling filter. They concluded that biological processes within the filter, rather than transport processes, were rate-limiting, and further, that biological reaction kinetics inside the biofilm were of zero order in the substrate concentration. While model results satisfactorily predict performance, substrate degradation rates were about one-eighth of those measured in parallel-suspended culture studies. Baltzis and Shareefdeen (1993) and Shareefdeen and Baltzis (1994) modeled the degradation of single and mixed pollutants (methanol, benzene, toluene) under steady-state conditions in a peat/pearlite biofilter. They assumed that the contaminants and oxygen were depleted in a fraction of the actual biolayer, termed an effective biolayer. In all three studies, reasonable fits to experimental data were obtained by adjusting rate-limiting parameters, such as mass transfer coefficients or biofilm surface area. None of these studies have incorporated the physiological response of the bacteria to hydrocarbon degradation-related stress. This stress response might be critical in assessing VPBR performance.

In the present investigation, kinetic and stoichiometric coefficients for toluene degradation and rates of injury and irreversible loss from suspended cell studies of *P. putida* 54G are combined with measured physical parameters such as Henry's law constant, biofilm surface area and biofilm-liquid interface thickness into a predictive VPBR model. Model results were compared with measured toluene degradation profiles in a flat plate VPBR at two different loading rates, 150 and 770 influent ppmv vapor phase toluene concentration. The model was fit to experimental results by adjusting only three parameters: intrinsic biomass density, death rate, and endogenous decay rate. Sensitivity analysis was conducted to identify those parameters that most affect the model results. This analysis provides a practical design tool for scale-up to bench and pilot-scale reactors.

Prior Experiments

Suspended culture studies were conducted to determine toluene degradation-associated injury on *P. putida* 54G (Mirpuri 1996). Bacterial stress or injury has been defined by McFeters

[1]Res. Mgr., 1345 Northland Dr., Basys Technologies, Mendota Heights, MN 55120. (612-683-8748; e-mail: rmirpuri@brauncorp.com)
[2]Analyst, Manufacturing Management Systems, Shell Services Co., Houston, TX 77077.
[3]Prof., Dept. d'Enginyeria Química, Escola Tècnica Superior d'Enginyeria Química, Universitat Rovira i Virgili, 43006 Tarragona, Spain.
[4]Assoc. Prof., CBE, Montana State Univ., Bozeman, MT 59717.
[5]Assoc. Prof., CBE, Montana State Univ., Bozeman, MT.
[6]Prof., CBE, Montana State Univ., Bozeman, MT.

Note. Associate Editor: Robert G. Arnold. Discussion open until November 1, 1997. To extend the closing date one month, a written request must be filed with the ASCE Manager of Journals. The manuscript for this paper was submitted for review and possible publication on May 13, 1996. This paper is part of the ***Journal of Environmental Engineering***, Vol. 123, No. 6, June, 1997. ©ASCE, ISSN 0733-9372/97/0006-0586–0592/$4.00 + $.50 per page. Paper No. 13239.

(1990) as the physiological, genetic, and structural consequences resulting from exposure to sublethal injurious environmental conditions and/or chemical agents. Results in our laboratories have shown that injury of *P. putida* 54G cells associated with toluene degradation increased with increase in toluene concentrations (Mirpuri 1996). These results were consistent qualitatively with research carried out by Leddy et al. (1995), who determined that Tol-variants of *P. putida* 54G were formed during toluene degradation. They suggested that the variants grew on other carbon sources such as organics leaking from injured cells and these variants continued to increase in numbers in the presence of toluene. Based on the injury studies, we concluded that the following three different cell phenotypes were found in suspended monocultures of *P. putida* 54G during toluene degradation:

1. Wild-type cells that degraded toluene and were uninjured—X^{++} cells
2. Cells that were reversibly injured and could grow on toluene only after resuscitation on rich medium—X^{+-} cells
3. Cells that irreversibly lost their toluene degrading capacity—X^{-} cells

Rates of formation of these cell types were determined by fitting a theoretical model to observed suspended culture results (Mirpuri 1996). The theoretical model was derived by assuming that

1. Growth of X^{+-} cells were negligible because they had to be resuscitated on rich mineral medium prior to degrading toluene.
2. The difference in the growth and decay of X^{++} cells was negligible in comparison to other processes that the injured cells undergo such as irreversible loss and injury.
3. The difference in growth rate and decay of X^{-} cells could be combined into one variable, μ'_{max}, which expresses the preference of the X^{-} cells for growth over decay.

Initial conditions used to solve the theoretical model (Mirpuri 1996) were as follows: at time $t = 0$, X^{+-} cells = X^{-} cells = 0, and X^{++} cells = X_0. X_0 are the maximum number of uninjured cells formed at the end of the logarithmic growth phase. The time scale was reduced by a day assuming that injury started at the end of the log-growth phase. Three parameters were evaluated: an injury coefficient (K_{INJ}) coefficient based on conversion of X^{++} to X^{+-} cells, an irreversible loss coefficient (K_{GL}) based on conversion of X^{++} to X^{-} cells, and finally, an estimate of the maximum specific growth rate of X^{-} cells (μ'_{max}). Values for these parameters are shown in Table 1 [detailed explanation in Mirpuri (1996)].

The injury studies (Mirpuri 1996) were conducted at two different influent gas-phase toluene concentrations, 150 ppmv and 770 ppmv, respectively. At the higher toluene concentration, a steady-state accumulation of benzyl alcohol, a toluene degradation product, was observed that indicated incomplete toluene degradation. The X^{-} cells were hypothesized to grow on organics leaking from injured cells and increase in number in the presence of benzyl alcohol (Leddy et al. 1995).

Henry's law constant for toluene was measured in batch reactors as 0.19 g m^{-3} toluene in air/g m^{-3} toluene (25°C, 0.82 atm) in water in comparison to a value of 0.271 (same units) published by Mackay et al. (1979). This value of Henry's law constant was calculated in equilibrium partitioning experiments for closed systems by varying toluene concentrations from 0 − 200 mg/l, using a procedure outlined by Gosset et al. (1985).

TABLE 1. Physical and Kinetic Parameters Used in AQUASIM to Model Flat Plate VPBR at 150 and 770 Influent Toluene Vapor Concentration

Description (1)	Units (2)	150 ppm (3)	770 ppm (4)
(*a*) Physical parameters			
Gas volume (V_G)	m^3	7.20E-04	7.20E-04
Liquid volume (V_L)	m^3	8.00E-05	8.00E-05
Total reactor volume (V)	m^3	8.00E-04	8.00E-04
Surface area (A)	m^2	0.02	0.02
Gas-liquid interfacial area (A_{GL})	m^2	0.02	0.02
Gas-liquid interface thickness (λ_{GL})	m	1.00E-05	1.00E-05
Liquid-biofilm interface thickness (λ)	m	2.50E-05	2.50E-05
Henry's law constant for toluene (H_T)	$g/m^{-3}/g/m^{-3}$	0.19	0.19
Henry's law constant for oxygen (H_O)	$g/m^{-3}/g/m^{-3}$	43.0	43.0
Density of biomass[a] (ρ_X)	g/m^{-3}	5.00E+04	5.00E+04
(*b*) Kinetic parameters			
Maximum specific growth rate (μ_{max})	d^{-1}	10.08	10.08
Toluene half-saturation constant (K_{ST})	g/m^{-3}	3.98	3.98
Oxygen half-saturation constant (K_{SO})	g/m^{-3}	0.025	0.025
Inhibition constant (K_I)	g/m^{-3}	42.78	42.78
Yield of biomass on toluene (Y_T)	g/g	0.86	0.86
Yield of biomass on oxygen (Y_O)	g/g	0.55	0.55
Endogenous yield on oxygen (Y_{Ob})	g/g	0.55	0.55
Injury rate (K_{INJ})	d^{-1}	0.06783	0.42696
Genetic loss rate (K_{GL})	d^{-1}	0.00655	0.06551
Net growth rate for X_n cells (μ_{net})	d^{-1}	0.02551	0.01182
Endogenous decay rate[a] (b_x)	d^{-1}	0.65	1.5
Death rate[a] (d_x)	d^{-1}	0.10	0.5

[a]Parameters represent coefficients adjusted to obtain best fit to total toluene degradation.

Short-term toluene degradation studies by *P. putida* 54G were conducted in batch cultures (Mirpuri 1996) by varying toluene concentration from 1 to 50 mg/l in the presence of excess oxygen, yielding the following relationship:

$$\mu = \frac{\mu_{max}\, T}{\left(K_{ST} + T + \dfrac{T^2}{K_I}\right)} \frac{O}{(K_{SO} + O)} \tag{1}$$

where μ = specific growth rate (d^{-1}); μ_{max} = maximum specific growth rate (d^{-1}); T = toluene concentration (g/m^{-3}); K_{ST} = toluene half-saturation constant (g/m^{-3}); K_I = substrate inhibition constant (g/m^{-3}); O = oxygen concentration (g/m^{-3}) and K_{SO} = oxygen half-saturation constant (g/m^{-3}). Values of cell yield were also determined from this data set. Values for all kinetic and stoichiometric parameters used are shown in Table 1.

EXPERIMENTAL METHODS

A flat plate VPBR was set up, as shown in Fig. 1. Our purpose in using a flat plate VPBR instead of a conventional

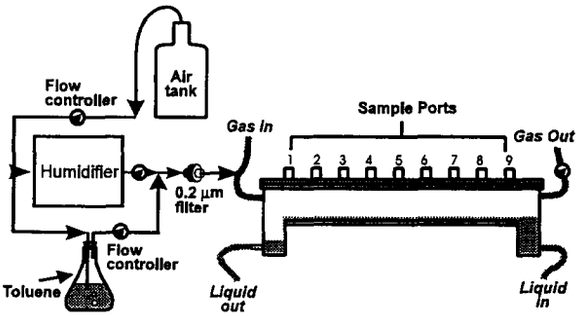

FIG. 1. Schematic of Experimental Flat Plate Reactor; Sample Ports Were Used to Collect Gas Phase and Liquid Phase Samples As Well As to Collect Dissolved Oxygen Profiles within Biofilm

biofilter with packing material is that it provides the opportunity to study a well defined system wherein biofilm surface area, liquid holdup, hydrodynamics, and other parameters can be determined accurately. In addition, it provides the opportunity for direct measurement of dissolved oxygen profiles and for determining liquid and biofilm mass transfer rates. Humidified toluene vapors were supplied at a flow rate of 50 ml/min in counter-current mode to liquid media flow at 1 ml/min. Liquid mineral salts media (denoted as HCMM2), which contained no organic compounds, was used as a source of inorganic nutrients with composition described by Ridgway et al. (1990). *P. putida* 54G biofilms grew on the bottom of the reactor (glass bottom) with toluene vapors being the only carbon and energy source. Two different experimental conditions were operated with influent toluene concentration of 150 and 770 ppmv, respectively. Headspace and liquid samples were collected everyday until the removal efficiency (defined as the % excess of influent over the effluent toluene concentration) was constant for 10 days, approximately thirty days from the start of the experiment. At the higher toluene concentration, theoretically, oxygen was stoichiometrically limiting (Williamson and McCarty 1976), while toluene was limiting at the lower concentration.

Sample ports at an influent and effluent position and along the lid of the reactor were provided as shown in Fig. 1. Toluene concentration in the gas phase was measured at the influent, effluent, and intermediate sample ports (2, 5, and 8), daily (in triplicate), throughout the duration of the experiment. 250 μl of headspace was injected into a HP 5890 Series II gas chromatograph equipped with an FID detector and an Alltech 0.1% A1-1000 Graphpac GC 80/100, 6 ft × 1/8 in. × 0.085 in., S.S. column (constant temperature of 140°C), operated in a splitless mode. The injector and detector were maintained at a constant temperature of 200°C and helium was used as the carrier gas at a flow rate of 30 ml/min.

Oxygen microsensors, fabricated as described in Lewandowski et al. (1991), with tips < 10 μm were inserted through sample ports 2, 5, and 8 to measure oxygen concentration profiles in the vapor, liquid, and biofilm phases. Oxygen concentration profiles [shown in Mirpuri (1996)] were used to estimate the gas-liquid, liquid-biofilm interface thickness and biofilm thickness. Slopes of the oxygen concentration profiles were measured in the absence and presence of toluene. Biomass yield and endogenous yield on oxygen were assumed to be related to the product of the ratio of the slopes (64%) and the actual yield of biomass on toluene [0.86, as reported in Mirpuri (1996)]. These values are presented in Table 1.

MODELING

Bulk Transport Reactions

The VPBR was divided into nine axial segments with the bulk gas, bulk liquid, and biofilm phases described separately. Mass balance equation for dissolved (D_i) and particulate (P_i) components, respectively, in the bulk liquid are

$$\frac{d(V_L C_{L,Di})}{dt} = Q_L(C_{L0,Di} - C_{L,Di}) + A_{LF} j_{L,Di} - A_{GL} j_{G,Di} + V_L r_{Di} \quad (2)$$

$$\frac{d(V_L C_{L,Pi})}{dt} = Q_L(C_{L0,Pi} - C_{L,Pi}) - A_{LF} j_{L,Pi} + V_L r_{Pi} \quad (3)$$

where C_{L0} = segment influent liquid phase concentration; C_L = bulk liquid concentration; j_L = mass flux per unit interfacial area across the biofilm-bulk liquid interface ($ML^{-2}t^{-1}$); j_G = mass flux per unit area across the gas-liquid interface; r = net production rate; V_L = bulk liquid volume; Q_L = liquid volumetric flow rate; A_{LF} = biofilm surface area of the segment; A_{GL} = bulk gas-bulk liquid interfacial area; and t = time.

Mass balance equation for dissolved components in the bulk gas is given by

$$\frac{d(V_G C_{G,Di})}{dt} = Q_G(C_{G0,Di} - C_{G,Di}) + A_G j_{GL,Di} \quad (4)$$

where C_{G0} = segment influent gas phase concentration; C_G = bulk gas concentration; V_G = bulk gas volume, and Q_G = gas volumetric flow rate. The biofilm-bulk liquid interfacial mass fluxes of dissolved and particulate components are, respectively

$$j_{L,Di}\lambda_L = D_{L,Di}(C_{FL,Di} - C_{L,Di}) \quad (5)$$

$$j_{L,Pi}\lambda_L = D_{L,Pi}(C_{FL,Pi} - C_{L,Pi}) \quad (6)$$

where λ_L = mass transfer boundary layer thickness across the biofilm-bulk liquid interface; D_L = liquid molecular diffusivity; and C_{FL} = concentration at the biofilm-bulk liquid interface.

The bulk gas-bulk liquid interfacial mass flux of dissolved components is given by:

$$j_{L,Di}\lambda_G = D_{G,Di}\left(C_{L,Di} - \frac{C_{G,Di}}{H_{Di}}\right) \quad (7)$$

where λ_G = mass transfer boundary layer thickness across the biofilm-bulk liquid interface, D_L = liquid molecular diffusivity; and C_{FL} = concentration at the biofilm-bulk liquid interface. The bulk liquid and bulk gas volumes are

$$V_L = V_C - V_F \quad (8)$$

where V_c = biofilm bulk liquid volume of the segment; and V_F = biofilm volume. The bulk gas volume, V_G, is constant.

Mass Transport and Biological Reactions within Biofilm

Wanner (1994) presented a mixed-culture biofilm model framework that describes biofilm processes of m bacterial species using n substrates. Wanner and Reichert (1995) presented the complete mathematical description for the mixed-culture biofilm model. In this study, several biological reactions are being considered, including growth of wild-type and Tol-variant cells, injury, variant formation, endogenous decay, and death. Table 2 shows the complete stoichiometry matrix and kinetic expressions for the various transformation processes considered in the model. Multiplying a rate (bottom row) by a coefficient above it in the matrix will give the rate of generation (positive) or use (negative) of that constituent by that process.

The first column in Table 2 denotes cell phenotypes and growth substrates that are simulated in the biofilm model. X^{++}, X^{+-}, and X^{-} cells have been described previously and represent cell phenotypes of *P. putida* 54G. T, O, and I represent concentrations of toluene, oxygen, and intermediates, respectively. The intermediates' concentration in the model represents a combination of dead or decaying cells, organics leaking from injured cells, and incomplete toluene degradation products such as benzyl alcohol (Mirpuri 1996).

SIMULATION

VPBRs were modeled using AQUASIM, a biofilm process simulation package (Reichert 1994b) capable of modeling any combination of mixed fluid reactors and mixed biofilm reactors. AQUASIM is also capable of modeling attachment, detachment, and advective transport of bacteria and substrates in liquid and biofilm phases. The flat plate VPBR was modeled using nine mixed reactors for the gas phase that were combined with nine biofilm reactors through diffusive links (Fig. 2). Reactors of the same type, i.e., gas or biofilm, were com-

TABLE 2. Biological Stoichiometry Matrix that is Used within AQUASIM to Describe Biofilm Process Occurring within VPBR. Multiplying Rate by its Appropriate Coefficient Gives Rate of Generation or Utilization (+ = Generation).

Species (1)	Process: Growth of X^{++} (2)	Injury (3)	Variant formation (4)	Growth of X^{-} (5)	Endogenous decay (6)	Death (7)
X^{++}	$+X^{++}$	$-X^{++}$	$-X^{++}$	—	$-X^{++}$	$-X^{++}$
X^{+-}	—	$+X^{++}$	—	—	—	$-X^{+-}$
X^{-}	—	—	$+X^{++}$	$+X^{-}$	$-X^{-}$	$-X^{-}$
T	$-X^{++}/Y_T$	—	—	—	—	—
O	$-X^{++}/Y_O$	—	—	$-X^{-}/Y_O$	$-(X^{++} + X^{-})/Y_{Ob}$	—
I	$+f_{tol}(X^{++}/Y_T)$	—	—	$-X^{-}/Y_I$	$+f_{cells}(X^{++} + X^{-})$	$+f_{cells}(X^{++} + X^{+-} + X^{-})$
Rate expression	$\mu_{max}\left[\frac{(T)}{(Ks_T + T + T^2/K_I)}\right]\left[\frac{(O)}{(Ks_O + O)}\right]$	K_{INJ}	K_{GL}	$\mu^{I}_{max}\left[\frac{(I)}{(Ks_I + I)}\right]\left[\frac{(O)}{(Ks_O + O)}\right]$	$b_X\left[\frac{(O)}{(Ks_O + O)}\right]$	d_X

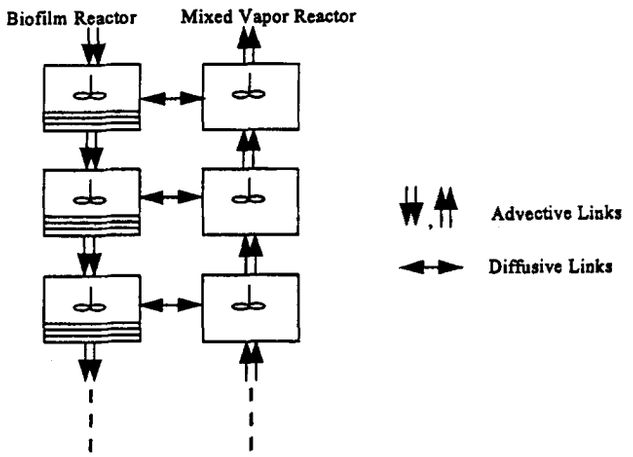

FIG. 2. Flow Schematic and Conceptual Reactor Configuration Used in AQUASIM Model; Nine of Each Reactor Type (Biofilm Reactor and Mixed Vapor Reactor) Were Used in Model

bined through advective links. Additional information on the model is available in Reichert (1994, 1995).

In the model, the contaminant is assumed to diffuse from the gas phase in a mixed vapor reactor (flowing countercurrent to the liquid phase) through a stagnant liquid layer into the biofilm phase where biological reaction occurs (denoted as a biofilm reactor). The following assumptions were made to simplify the model:

- Growth and injury kinetics determined for suspended cells of *P. putida* 54G were valid for biofilm cells of the same bacteria.
- Bulk gas and bulk liquid phases are well mixed.
- Water volume fraction in the biolayer was constant, and only growth resulted in an increase in biofilm thickness.
- Published values of Henry's law and half-saturation coefficients for oxygen were valid for the present system.
- Biofilm density was constant throughout the reactor.
- Planar geometry.
- Diffusivity in biofilm was constant (=0.8 × diffusivity in water).

The model was used to evaluate steady-state toluene degradation and oxygen consumption within the biofilm, as well as biofilm thickness values at different positions in the flat plate. Values of parameters, shown in Table 1, along with an influent vapor phase toluene concentration (150 or 770 ppmv), were input into the model.

SENSITIVITY ANALYSIS

Sensitivity analyses using the computational model are of critical importance to the design of any experimental program and for determination of rate-limiting steps and process parameters that may be important to scale-up. AQUASIM uses the following expression, described in greater detail in Reichert (1994b), to evaluate the sensitivity of a function, such as toluene degradation rate in our case, to different parameters:

$$\delta_{f,p} = \frac{f\,\partial p}{p\,\partial f} \tag{9}$$

where sensitivity index, $\delta_{f,p}$, = relative change in function p for a relative change in parameter f, calculated as a linear approximation. Because the sensitivity index is normalized, it does not depend on the units of the parameter used, and direct comparisons of sensitivity can be made. The advantage of using such a function is that sensitivity of toluene degradation rates to both experimentally and theoretically determined parameters can be compared and can be used to assess potential applications of AQUASIM for predicting performance of bench and pilot-scale VPBRs.

RESULTS AND ANALYSIS

Table 3 shows a comparison of toluene degradation profiles experimentally determined in the flat plate VPBR and results calculated using AQUASIM. The model results match the experimental values of toluene degradation at different points along the length of the reactor, as well as total toluene degradation calculated in g d^{-1}. The experimental results exhibit significant gradients along the length of the VPBR, which in part, justifies the computational complexity of nine reactors in

TABLE 3. Results of Comparative Study of Experimentally Determined Toluene Degradation in Flat Plate VPBR and Results Calculated from VPBR Model

Experiment conducted (1)	Experimental (2)	Calculated (3)	Units (4)
(*a*) 150 ppm experiment			
Influent	152.00 ± 5.6	152.00	ppm
Port 2	123.00 ± 5.2	125.90	ppm
Port 5	94.00 ± 4.7	94.07	ppm
Port 8	74.00 ± 3.9	69.39	ppm
Effluent	59.00 ± 4.2	57.86	ppm
Toluene degradation rate	0.0212	0.0214	g/d^{-1}
(*b*) 770 ppm experiment			
Influent	767.00 ± 32.2	767.00	ppm
Port 2	642.00 ± 39.3	683.20	ppm
Port 5	475.00 ± 29.5	564.80	ppm
Port 89	425.00 ± 38.2	451.90	ppm
Effluent	363.00 ± 29.2	383.00	ppm
Toluene degradation rate	0.0920	0.0874	g/d^{-1}

TABLE 4. Sensitivity Analysis Conducted on Select Parameters Using AQUASIM for Modeling Flat Plate VPBR

Flat Plate VPBR	152 ppm		767 ppm	
Description (1)	S.I. (%) (2)	Rank (3)	S.I. (%) (4)	Rank (5)
Surface area (A)	0.500	2	1.634	1
Gas-liquid interfacial area (A_{GL})	—	—	—	—
Gas-liquid interface thickness (λ_{GL})	—	—	—	—
Liquid-biofilm interface thickness (λ)	−0.097	6	−0.063	9
Henry's law constant for toluene (H_T)	−0.577	1	−0.459	3
Henry's law constant for oxygen (H_O)	—	—	−0.167	4
Density of biomass (ρ_X)	—	—	—	—
Maximum specific growth rate (μ_{max})	0.197	4	0.144	5
Toluene half-saturation constant (K_{ST})	−0.167	5	−0.085	7
Oxygen half-saturation constant (K_{SO})	—	—	—	—
Inhibition constant (K_I)	—	—	—	—
Yield of biomass on toluene (Y_T)	−0.203	3	−0.462	2
Yield of biomass on oxygen (Y_O)	—	—	0.097	6
Endogenous yield on oxygen (Y_{Ob})	—	—	0.059	10
Injury rate (K_{INJ})	−0.026	7	−0.026	12
Genetic loss rate (K_{GL})	—	—	—	—
Net growth rate for X_n cells (μ_{net})	—	—	—	—
Endogenous decay rate (b_X)	0.0146	9	0.050	11
Death rate (b_X)	0.0149	8	0.069	8

Note: Sensitivity index (S.I.) (%), evaluated in the table denotes the percent change in toluene degradation (g d^{-1}) when a particular parameter is changed by 1%—represents a negligible effect of that parameter on toluene degradation.

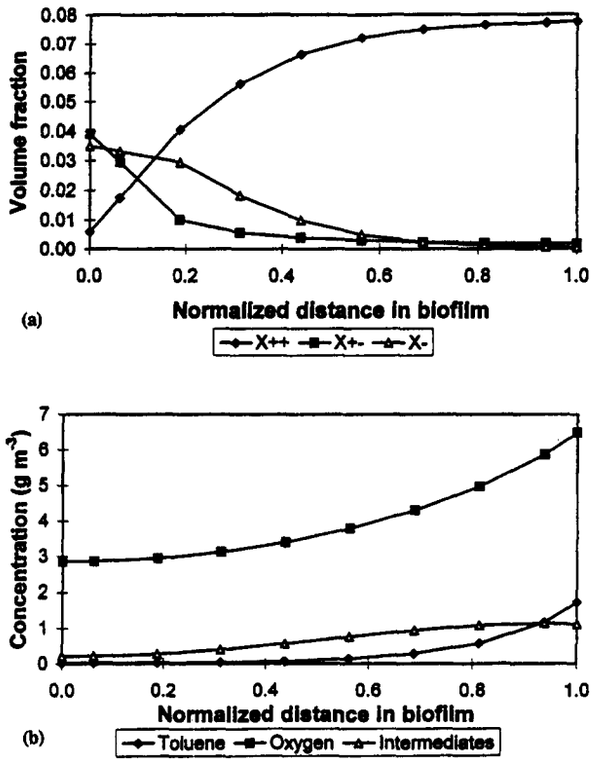

FIG. 3. Model-Predicted Profiles: (a) Fraction of Each Cell Type within Biofilm; (b) Concentrations of Toluene, Dissolved Oxygen and Intermediates within Biofilm at Influent Gas Phase Toluene Concentration of 150 ppmv

series in AQUASIM. Increasing the toluene concentration by a factor of five led to approximately a five-fold increase in toluene degradation. Due to the reactor geometry and extremely low fluid shear, the biofilm reached a climax thickness of over 2 mm, and had a very loose and "fluffy" structure. Mass transport limitations as a result of the thick biofilm were expected. Nevertheless, toluene degradation efficiencies were about 62 and 53%, at 150 and 770 ppmv influent toluene concentration, respectively, and suggest satisfactory performance with regard to toluene degradation.

Sensitivity indexes from analyses conducted on toluene degradation rates (g/d^{-1}), as affected by physical and kinetic parameters for both experimental conditions are shown in Table 4. The negative sign associated with the sensitivity index indicates that, as the parameter under consideration increases, toluene degradation decreases. Henry's law constant for toluene (H_T), biomass yield on toluene (Y_T), and biofilm surface area (A) were determined to be the most important parameters affecting predictions of toluene degradation. The first two parameters were measured independently in previous experiments and the area was evaluated from flat-plate geometry (Mirpuri 1996).

In comparison to the 150 ppmv experiment, sensitivity analyses during the 770 ppmv experiment suggest that accurate estimates of yield on toluene (Y_T) are necessary. Also, modeling results from the higher toluene concentration suggest an increasing dependency on oxygen-related parameters (Y_O, Y_{Ob}, and H_O). This makes sense, since at the higher toluene concentration, oxygen is stoichiometrically limiting. The kinetic coefficients, μ_{max} and K_{ST} are also important parameters for predicting toluene degradation. This system may therefore be reaction rate-limited rather than diffusion rate-limited. Baltzis and Shareefdeen (1994) similarly concluded that the biolayer surface area per unit volume of reactor was the most sensitive parameter in their model. The sensitivity analysis indicated that both death and endogenous decay rate (b_x and d_x) increased with toluene concentration (Table 1). However, all three parameters that were adjusted to fit the VPBR model to experimental results (D_X, b_X, and d_X) showed a weak effect on toluene degradation. This increases the confidence of our model substantially because none of the estimated parameters affected toluene degradation.

Figs. 3 and 4 show the model prediction of gradients in cell types and in dissolved constituents within the biofilm for the 150 ppmv and 770 ppmv cases, respectively. For both cases, the X^{++} cells decrease from the biofilm surface toward the substratum, while X^{-} cells are low near the surface and increase significantly toward the base of the biofilm. X^{+-} cells are located throughout the biofilm, but increase slightly toward the substratum. Comparing the dissolved species concentration profiles, the toluene and oxygen profiles behave predictably; toluene is depleted first at low concentration (Fig. 3) while oxygen is depleted first at the higher toluene concentration (Fig. 4). The most significant difference between Figs. 3 and 4 is the concentration of metabolic intermediates. At 150 ppmv, sufficient oxygen exists throughout the biofilm to allow the X^{-} cells to remain active, so that most of the intermediates formed could diffuse toward the substratum and be degraded. At 770 ppmv, however, oxygen is depleted within the film, effectively halting the degradation of the intermediates. It can be seen from the slopes of the intermediate profile in Fig. 3 that intermediates left the film and infused inward at approximately equal rates.

These predictions are consistent with experimental results from performing physiological staining techniques on biofilm samples taken from the flat plat reactor. Those results demonstrated that respiratory activity in the bottom 50 μm or so was most significant in the basal 5 μm (Mirpuri 1996). Leddy et al. (1995) have hypothesized that Tol-variants form when wild-type cells are exposed to toluene and that the variants grow on intermediates produced as a result of incomplete toluene degradation. They have also shown that benzyl alcohol, a toluene degradation intermediate, drives the formation of the variants. Results in our laboratories have shown accumulation of benzyl alcohol in suspended cultures of *P. putida* 54G cells

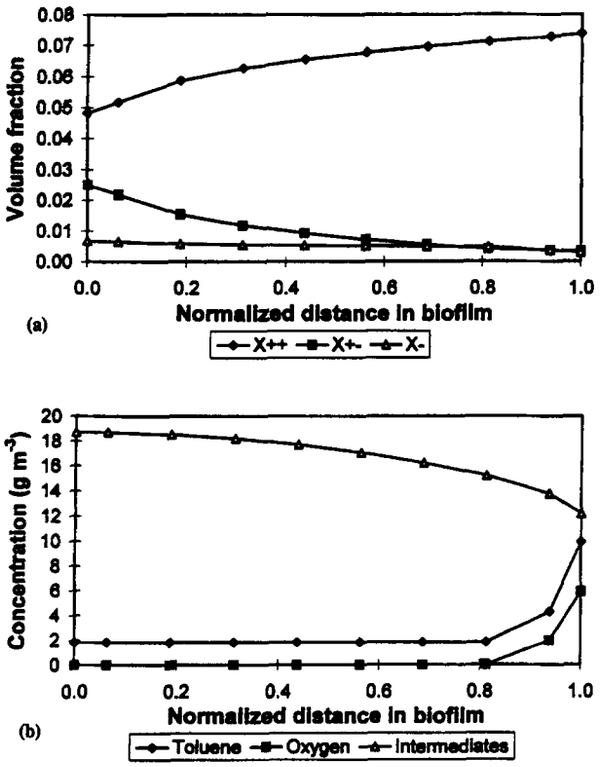

FIG. 4. Model-Predicted Profiles: (a) Fraction of Each Cell Type within Biofilm; (b) Concentrations of Toluene, Dissolved Oxygen and Intermediates within Biofilm at Influent Gas Phase Toluene Concentration of 770 ppmv

growing on toluene (Mirpuri 1996). Because the X^- cells (putative Tol-variants) cannot grow on toluene, but grow on endogenous substrates (incomplete toluene degradation products, as well as dead and decaying cell matter), most of the X^- cells stratify at the base of the biofilm in a region where toluene concentration is the lowest. Injured cells (X^{+-}) are formed from wild-type cells as a result of toluene exposure, and only undergo death and decay afterward. These are left behind as the film grows outward, and are protected from detachment by the continually growing outer layer.

Having developed this scenario, it was somewhat disappointing to us that the parameters K_{INJ}, μ^I_{max}, and K_{GL} showed a negligible effect on toluene degradation (Table 4). Our explanation for this lack of sensitivity is that sufficient competent wild-type cells exist at the top of the biofilm (Figs. 3 and 4) to act effectively as an active biolayer of 200 μm or so, regardless of the stratification below. It does, however, serve as a warning that a significant sloughing event could remove the most of the population degrading the target compound in a biofilter, causing long recovery times.

CONCLUSIONS AND FUTURE WORK

In this study, toluene degradation in a flat plate VPBR was modeled using AQUASIM and predicted results were compared with experimental observations. Based on this study

1. A reasonable fit was attained between experimental observations and predicted results for toluene uptake rate and toluene concentration profiles in a flat plate VPBR.
2. Values for biofilm surface area, Henry's law constant for toluene and biomass yield on toluene significantly affected toluene degradation for both experimental conditions.
3. At a high toluene concentration, toluene degradation was affected by oxygen-related parameters such as endogenous yield on oxygen, Henry's law constant for oxygen, and yield of biomass an oxygen.
4. Qualitatively, the model can be used to study stratification of cell physiological states in VPBR biofilms.

These results provide a framework for using fundamental information from suspended culture studies and from ideal reactors to calibrate a phenomenological VPBR model that can then be used to predict performance of such reactors. While these results are heartening, it would be imperative to determine if such an approach is feasible in scaling to nonideal column VPBRs at the bench and pilot scale.

ACKNOWLEDGMENTS

This work was supported by the Center for Biofilm Engineering at Montana State University, a National Science Foundation-sponsored engineering research center (cooperative agreement EEC-8907039), Orange County Water District, and National Water Research Institute. We would like to thank Peter Reichert (Swiss Federal Institute Environmental Science and Technology, Dubendorf, Switzerland) for technical assistance with the AQUASIM model, and Harry Ridgeway (Orange County Water District, Fountain Valley, CA), and Gordon McFeters (Montana State University, Bozeman, MT) for their thoughtful insights on the topic of physiological stress and injury.

APPENDIX I. REFERENCES

Baltzis, B. C., and Shareefdeen, Z. (1993). "Modeling and preliminary design criteria for packed-bed biofilters." *Proc., 86th Meeting, Air and Waste Mgmt. Assn.*.

Diks, R. M. M., and Ottengraf, S. P. P. (1991). "Verification studies of a simplified model for the removal of dichloromethane from waste gases using a biological trickle filter—Part I." *Bioprocess Engrg.*, 6, 93–99.

Gosset, J. M., Cameron, C. E., Eckstrom, B. P., Goodman, C., and Lincoff, A. H. (1985). "Mass transfer coefficients and Henry's constants for packed-tower air stripping of volatile organics: Measurements and correlation." *Final Rep.*, Air Force Engineering and Services Center, Tyndall Air Force Base, Fla.

Leddy, M. B., Phipps, D. W., and Ridgway, H. F. (1995). "Catabolite-mediated mutations in alternate toluene degradation pathways in *Pseudomonas putida*." *J. Bacteria*, 177, 4713–4720.

Leson, G., and Winer, A. M. (1991). "Biofiltration: An innovative air pollution control technology for VOC emissions." *J. Air Waste Mgmt. Assn.*, 41, 1045–1054.

Lewandowski, Z., Walser, G., and Characklis, W. G. (1991). "Reaction kinetics in biofilms." *Biotech. Bioengrg.*, 38, 877–882.

Mackay, D., Shiu, W. Y., and Sutherland, R. P. (1979). "Determination of air-water Henry's law constants for hydrophobic pollutants." *Envir. Sci. Technol.*, 13, 333–337.

McFeters, G. A. (1990). "Enumeration, occurrence, and significance of injured indicator bacteria in drinking water." *Drinking water microbiology: Progress and recent developments*, G. A. McFeters, ed., Springer-Verlag, New York.

Mirpuri, R. (1996). "Physiological and environmental factors affecting biofilm formation and activity in vapor phase bioreactors," PhD dissertation, Montana State University, Bozeman, Mont.

Reichert, P. (1994a). "AQUASIM—A tool for simulation and data analysis of aquatic systems." *Water Sci. and Technol.*, 30, 21–30.

Reichert, P. (1994b). "Concepts underlying a computer program for the identification and simulation of aquatic systems." *Schriftenreihe der EAWAG No. 7*, Swiss Federal Institute for Environmental Science and Technology, CH-8600, Dubendorf, Switzerland.

Reichert, P. (1995). "The use of AQUASIM for estimating parameters for activated sludge models." *Water Sci. Technol.*, 31, 135–147.

Ridgway, H. F., Safarik, J., Phipps, D., Carl, P., and Clark, D. (1990). "Identification and catabolic activity of well-derived gasoline-degrading bacteria from a contaminated aquifer." *Appl. Envir. Microbiology*, 56, 3565–3575.

Shareefdeen, Z., and Baltzis, B. C. (1994). "Biofiltration of toluene vapor under steady-state and transient conditions: theory and experimental results." *Chemical Engrg. Sci.*, 49, 4347–4360.

Wanner, O. (1994). "Modeling of mixed-population biofilm accumulation." *Biofouling and biocorrosion in industrial water systems*, C. G. Geesey, Z. Lewandowski, and H. C. Flemming, eds., Lewis, Ann Arbor, Mich.

Wanner, O., and Reichert, P. (1995). "Mathematical modeling of mixed-culture biofilms." *Biotechnol. Bioengrg.*, 49, 172–184.
Williamson, K., and McCarty, P. L. (1976). "Verification studies of the biofilm model for bacterial substrate utilization." *J. Water Pollution Control Fed.*, 48, 281–296.

APPENDIX II. NOTATION

The following symbols are used in this paper:

A = biofilm surface area (m^2);
A_{GL} = bulk gas-bulk liquid interfacial area (m^2);
b_X = endogenous decay rate (d^{-1});
C_G = bulk gas concentration (g/m^{-3});
$C_{L,Dl}$ = bulk liquid concentration for dissolved components (g/m^{-3});
C_{LO} = segment influent liquid phase concentration (g/m^{-3});
$C_{L,Pl}$ = bulk liquid concentration for particulate components (g/m^{-3});
D_G = gas diffusivity (m^2/d^{-1});
D_L = liquid diffusivity (m^2/d^{-1});
d_X = death rate (d^{-1});
f = diffusivity in biofilm/diffusivity in water;
f = parameter on which sensitivity analysis is based;
f_{cells} = fraction of cells converted via death and endogenous decay;
f_{tol} = fraction of toluene converted to intermediates via incomplete biodegradation;
H_O = Henry's law constant for oxygen (g/m^{-3} air/g/m^{-3} water);
H_T = Henry's law constant for toluene (g/m^{-3} air/g/m^{-3} water);
j_G = mass flux per unit interfacial area across gas-liquid interface ($g/m^{-3}/d^{-1}$);
j_L = mass flux per unit interfacial area across biofilm-liquid interface ($g/m^{-3}/d^{-1}$);
K_{GL} = irreversible loss rate (d^{-1});
K_I = inhibition constant (g/m^{-3});
K_{INJ} = injury rate (d^{-1});
K_{SO} = oxygen half-saturation constant (g/m^{-3});
K_{ST} = toluene half-saturation constant (g/m^{-3});
p = function used in AQUASIM for sensitivity analysis;
Q_G = gas volumetric flow rate (m^3/d^{-1});
Q_L = liquid volumetric flow rate (m^3/d^{-1});
r = net production rate (g^{-3}/d^{-1});
t = time (d^{-1});
V_C = biofilm + liquid volume (m^3);
V_F = biofilm volume (m^3);
V_G = gas volume (m^3);
V_L = liquid volume (m^3);
X^{++} = wild-type cell concentration (g/m^{-3});
X^{+-} = injured cell concentration (g/m^{-3});
X^- = nontoluene-degrading cell concentration (g/m^{-3});
Y_I = yield of X^- biomass of intermediates (g biomass/g intermediates);
Y_O = yield of biomass on oxygen (g biomass/g oxygen);
Y_{Ob} = endogenous yield on oxygen (g biomass/g oxygen);
Y_T = yield of biomass on toluene (g biomass/g toluene);
$\delta_{f,p}$ = sensitivity index on a normalized scale used in AQUASIM;
λ_{LF} = biofilm-liquid interface thickness (m);
λ_{GL} = gas-liquid interface thickness (m);
μ = specific growth rate (d^{-1});
μ_{max} = maximum specific growth rate (d^{-1});
μ'_{max} = maximum specific growth rate for X^- cells (d^{-1}); and
ρ_x = biomass density ($g\ m^{-3}$).